

# Strain Based Design—What the Contribution of a Pipe Manufacturer Can Be

Andreas Liessem  
Europipe GmbH  
Mülheim, Germany

Gerhard Knauf, Steffen Zimmermann  
Salzgitter Mannesmann Forschung GmbH  
Duisburg, Germany

## ABSTRACT

Exploration of new energy resources located in areas of complex ground and ambient climate imposes strict requirements on pipeline material and design. One of the major research issues in such areas is differential ground movement, which, possibly, is associated with large longitudinal straining in addition to plastic circumferential elongation. Hence, common design principles need thorough re-consideration, notably with respect to strain hardening properties of both base metal and girth welds. This paper summarizes results of a research, which was conducted within Europipe GmbH and supported by Salzgitter Mannesmann Forschung GmbH. Central to the discussion is the numerical representation of strain hardening behavior of pipeline steels, which mainly was focused on base metal. In particular, the discussion comprises stress-strain behavior in transverse as well as in longitudinal direction, the effect of material ageing and the significance of uniform elongation.

**KEY WORDS:** Strain hardening; design; uniform elongation; power law; true stress-true strain; engineering stress-engineering strain, UOE line pipe.

## INTRODUCTION

With the sustained rise in both oil and gas price to record levels, hydrocarbon reserves that were considered too expensive to justify production only a few years ago are now being considered as attractive. Fortunately, advances in technologies for exploration and production do allow uneconomic reserves to be accessed (Martin, 2006). These “new” reserves tend to be in regions where difficult ground prevails. That is to say, more and more pipelines will be prone to large differential ground movements. Differential ground movements may have many reasons such as soil subsidence, frost heave, thaw settlement and landslides, to name a few. A phenomenon, which is common to such load scenarios, is that they may evoke large longitudinal strains in addition to plastic circumferential elongation. This is very much different to the case of bare pressure containment where, mainly, circumferential and radial components of strain tensor undergo plastic deformation. Since longitudinal strains may be tensile or compressive complex multi-axial stress states accrue with plastic deformation

developing in more than two co-ordinate directions, which, within a cross section, are not uniform any more. This imposes strict requirements on pipeline material and design. It appears that at least two parties can actively contribute to safe and reliable energy transportation solutions. While pipeline operators are responsible to deliver appropriate designs across well-balanced and rational principles pipe manufacturers are requested to supply advanced material solutions prone to fulfill what has been assumed during the design process. The possible contribution of pipe manufacturers in this context is one subject of the present paper.

In order to ensure pipeline safety, integrity and environmental impact an alternative design methodology, Strain Based Design, may serve as the key to such difficult pipeline applications (Mohr, 2006, Zhou et al. 2006). This is because loading in the sense of Strain Based Design tends to apply a given displacement rather than force to the pipeline. Most often, such displacements impose a radius of curvature to the pipeline, a result of which is a bending moment, see Fig. 1.

Meanwhile Strain Based Design is addressed in a number of design codes, e. g. CSZ Z662-03 (CSZ Z662-03 2003). Still, these do not give sufficient guidance as regards pipeline structural analysis. In principle, the methodology of Strain Based Design is developed in connection with the philosophy of Limit State Design, where it stands for a specific subset of limit states where displacement controlled loads dominate the mechanical pipeline response. In Limit State Design the design value of load action  $S_d$  is compared to the design value of the resistance side (material)  $R_d$ :

$$S_d \leq R_d \quad (1)$$

Therein,  $S_d$  is the sum of all individual load contributions multiplied by partial (safety) factors  $\gamma_{s,i} \geq 1.0$ :

$$S_d = \sum \gamma_{s,i} s_i, \quad (2)$$

with  $s_i$  being individual load contributions. The design value of the resistance is defined as the quotient of nominal (or “characteristic”) resistance  $R$  and the partial (safety) factor  $\gamma_R \geq 1.0$ :

$$R_d = \frac{R}{\gamma_R}. \quad (3)$$

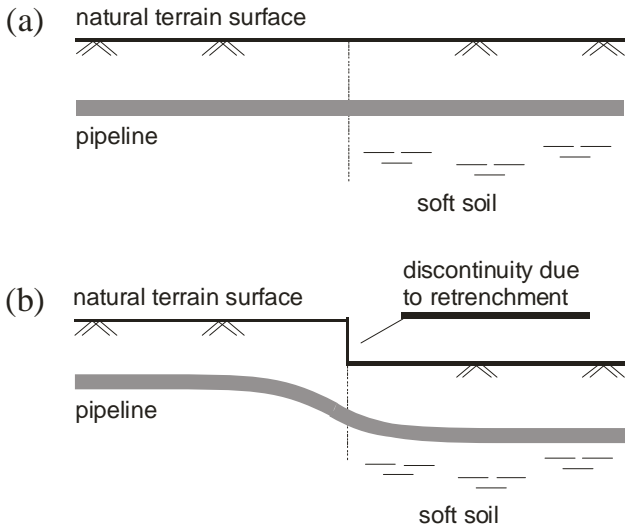


Fig. 1: Typical Strain Based Design situation.

Partial factors  $\gamma_{S,i}$  and  $\gamma_R$  represent the statistical scatter of both action side and resistance side and, hence, will be generally different. In view of Strain Based Design, safety is established on basis of the variability associated with the strain demand given by design requirements on one hand and strain capacity, which is intrinsic to the pipeline steel on the other hand. To be specific, a limit state condition can be expressed as follows (Zhou et al. 2006):

- factored (increased) maximum tensile strain demand  $\leq$  factored (reduced) tensile strain capacity
- factored (increased) maximum compressive strain demand  $\leq$  (reduced) compressive strain capacity

Although the input of pipe manufacturers usually starts early in the design process, this is the point where information on strain capacity becomes critical. Strain capacity expresses in the material's stress-strain curve or, more briefly, in its uniform elongation. Hereinafter, it is delineated what a pipe manufacturer can do in order to actively support decision-making, that is to say to support weighing out the pros and cons of a specific on-shore line pipe solution. Although in many articles the notion of Strain Based Design is put forward closely associated with longitudinal strain, here, Strain Based Design will be understood in a much more general sense. Thus, discussion of "engineering" strain capacity will not be delimited to axial strain but will comprise circumferential elongation and, thus, transversal stress-strain behavior as well. Attention is directed mainly to tensile strain capacity and mathematical representation thereof.

Because line pipe is subjected to thermal treatment within most anti-corrosion coating processes carbon line pipe naturally undergoes some sort of thermal ageing. Normally, the effect of thermal ageing is not taken into account, neither in material characterization nor in the design itself. Besides, any carbon steel line pipe is subjected to an ongoing natural ageing process in the course of its operation time following Arrhenius' equation changing yield-to-tensile ratio, uniform elongation and strain hardening exponent from possibly good to worse. For this reason, also the effect of ageing on stress-strain data was investigated, illustrating the shift of material behavior qualitatively as well as quantitatively. For example, Fig. 2 shows the effect of ageing on yield-to-tensile ratio, stress-strain behavior and uniform elongation of a grade X70 line pipe steel.

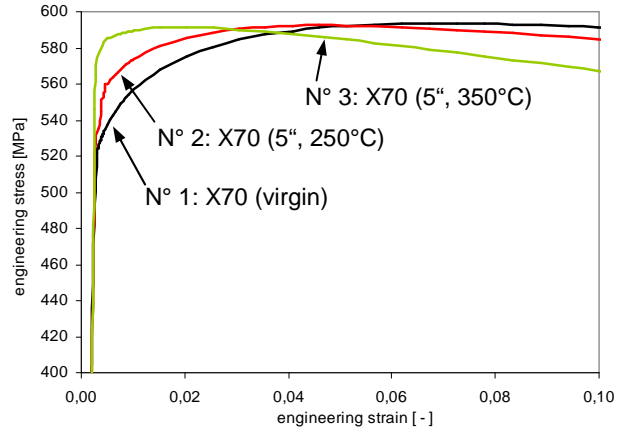


Fig. 2: Effect of thermal ageing on stress-strain curve in transverse direction and on uniform elongation.

Stress-strain curve N° 1 corresponds to the virgin material before artificial ageing. Graph 2 and 3 represent the same material after some time of artificial ageing (thermal treatment). While identical holding times were used (5") the temperatures were T (graph 2) and 1.4T (graph 3) respectively. In the present case, uniform elongation reduced by 25 (curve 2) and 68% (curve 3) as compared to graph N° 1 while corresponding yield-to-tensile ratio  $Y/T$  increased by 6 and 10% respectively.

## STRAIN CAPACITY OF PIPELINE: THEORETICAL BACKGROUND

This section is devoted first to "Classical Strain Based Design" as it is described in most references, focusing on axial strain only. Basically, the tensile strain limit of a pipeline is determined by the behavior of girth weld flaws in response to applied external strain. The basic approach is based on the inter-relationship between longitudinal pipe stress-strain properties, axial toughness and stress-strain properties of the weld and heat affected zone, flaw size and its location within the weld as well as the applied load.

Typical assessment following a strain based method of analysis requires plastic collapse limits to be understood as a function of the relationship between the pipe/weld properties and flaw size. If weld flaws are small and the weld metal strength over-matches base metal strength and reasonable fracture toughness is present, then large tolerable strains can be accommodated in the pipeline. In so doing, applied displacements are transmitted to the pipe and strain, preferentially, develops in the base material. Consequently, the weld is shielded off from large plastic strains (Zhou et al., 2006). In other words, weld and heat affected zone do not need to develop significant strain in order to follow strain-induced movements of the substrate.

Adequate yield-to-tensile ratio  $Y/T$ , sufficient uniform elongation  $\epsilon_{UTS}$  and shape of stress-strain curve of pipe base material may actively be in support of straining happening in the pipe rather than in girth welds or heat affected zone. From the above, it becomes apparent that the pipe must have ample strain capacity in order to be able to locally accommodate large axial strain and, at the same time, to allow for development of sufficient circumferential elongation. The latter especially gains importance when implementing high-grade material (greater than or equal X80) where, similarly, longitudinal welds tend to absorb a large portion of strain.

Usually, interaction of pipe and weld stress-strain behavior are analyzed using the finite element method (Zhou et al., 2006, Bowker et al., 2006). This requires stress-strain information be readily available in numerical format. That is to say, experimental stress-strain information upraised on tensile coupons is to be represented by means of adequate analytical approaches, in most of the cases being approximations of the power law type.

## MATHEMATICAL REPRESENTATION OF STRESS-STRAIN BEHAVIOR

### General

In recent years, within Europipe GmbH significant efforts have been undertaken in order to assess stress-strain behavior of UOE line pipe. Motivated by the fact that with increasing steel grade (material) and, with it, circumferential elongation (structure) is gradually decreasing, first, a huge research campaign was conducted in order to assess stress-strain data in transverse direction including thermal ageing effects. Besides, part of this information was critical for optimizing forming processes within Europipe production route. Stimulated by customer requests and the general development targeting at Strain Based Design approaches, this was then followed by a campaign, which has been directed towards axial stress-strain behavior and which still is in progress. In both campaigns a total of four modeling approaches were applied to experimental data and thoroughly analyzed, the individual approaches being:

- Hollomon (1949)
- Ludwik (1909)
- Swift 1952, mentioned in Thomas (2001)
- Ramberg Osgood (1943)

While the first three approaches are representations of true stress-true strain information, the latter one is capable of representing engineering stress-strain data.

Furthermore, a prediction method has been developed enabling fast assessment of strain hardening exponents of Hollomon type in terms of  $Y/T$ . Currently, the method is limited to evaluating strain hardening exponents of stress-strain behavior in transverse direction. However, it is the intent to extend this tool for longitudinal stress-strain behavior in the near future.

This is particularly interesting because, in early stages of design, stress-strain data is frequently unavailable. Comparison with results from best fit analysis shows that the approximate expression for strain hardening exponent calculation is simple to operate and efficient for a wide range of pipeline steel material.

### Constitutive Equations for Representing Strain Hardening

For representing constitutive behavior up to strains smaller than or equal the uniform elongation a large variety of approaches are available in the literature, see above. The abovementioned models were selected under the premise of taking care that these have relevance for engineering practice. Most simply, material behavior is described by empirical relationships. All equations to be introduced below will represent material behavior, and strain hardening behavior in particular, solely by mere mathematical treatment. Hence the equations are empirical in nature and, thus, do not resort to the causes encountered on micro-structural level.

Deformations in metal and steel are usually large, notably close to the ultimate failure event. Resorting to this observation, Ludwik (1909) postulated that small elastic strains could be considered as negligible. He then proposed a power law representing purely plastic behavior. The power law takes the form:

$$\sigma = C_0 + C_L \varepsilon^{n_L} \quad (4)$$

where, initially,  $C_0$  was conceived as the onset of yielding, namely as yield strength. However, it has proved to be inconvenient to choose the parameter  $C_0$  as the yield strength because the power law curve might deviate substantially from the stress-strain graph to be represented, such that the representation becomes inaccurate.  $C_L$  is the Ludwik stiffness parameter and  $n_L$  the Ludwik strain hardening exponent.

Hollomon (1945) sought for a simpler expression by waiving the parameter  $C_0$ :

$$\sigma = C_H \varepsilon^{n_H} \quad (5a)$$

It is important to notice that the stiffness parameter  $C_H$  in Eq. (5a) is not identical to the one of Eq. (4). Unlike the Ludwik strength parameter  $C_L$  the Hollomon strength parameter  $C_H$  can be directly associated with the ultimate engineering strength  $\sigma_{UTS}$  of the material.  $C_H$  is calculated as:

$$C_H = \left( \frac{e}{n_H} \right)^{n_H} \sigma_{UTS} \quad (5b)$$

where  $e = 2.178\dots$  is the natural number. In the range of large strains, the Ludwik power law (4) does not fit experimental data any better than it is achieved by using Eq. (5). A representation, which accounts for possible pre-straining is the one of Swift dating back to 1952 (Thomas, 2001):

$$\sigma = C_S (\varepsilon_0 + \varepsilon)^{n_S} \quad (6)$$

where  $C_S$  and  $n_S$  are, again, stiffness parameter and strain hardening exponent respectively. The idea of introducing a residual strain, which might be left over from cold forming, is interesting notably in the context of UOE pipe production. One may think, for instance of plastic strains evoked in the O-forming or the expansion procedure.

The formulae introduced above do not consider the elastic branch of the stress-strain diagram. Nevertheless, this part of the constitutive relation may become important when dealing with sheet forming as encountered in the production of UOE pipes. Although large deformations are prevailing when forming sheet, generally, residual stresses are induced, causing spring-back behavior. This is detrimental because spring-back commonly entails significant deviations from the shape, which is actually targeted at. Likewise, it is reasonable to account for the elastic contribution when designing according to Strain Based Design principles because the notion of Strain Based Design does not encompass strains greater than approximately 2%. Within this range the elastic contribution might contribute to a significant amount to total strain.

The linear elastic branch of the stress-strain diagram can be taken into account by superposing elastic and plastic strain contributions as proposed as early as 1943 by Ramberg & Osgood:

$$\varepsilon^* = \frac{\sigma^*}{E} + \varepsilon_p^* \left( \frac{\sigma^*}{\sigma_p^*} \right)^{n_{RO}} \quad (7a)$$

Therein,  $E$  is the elastic modulus and  $\sigma_p^*$  is a "proof stress". Commonly, the proof stress is conveniently chosen either as  $R_{p0.1}$ ,  $R_{p0.2}$ , or, if applicable, as  $R_{t0.5}$ . The strain  $\varepsilon_p^*$  corresponds to the plastic strain correlating with  $R_{p0.1}$  or  $R_{p0.2}$ . The strain hardening exponent  $n_{RO}$  is determined by fixing the plastic part of the Ramberg-Osgood curve at

the technical yield point ( $\varepsilon_y^* | \sigma_p^*$ ) and requiring that it passes through the ultimate point ( $\varepsilon_{UTS}^* | \sigma_{UTS}^*$ ). Thus,

$$n_{RO} = \frac{\ln \left[ \frac{1}{\varepsilon_y^*} \left( \varepsilon_{UTS}^* - \frac{\sigma_{UTS}^*}{E} \right) \right]}{\ln \left( \frac{\sigma_{UTS}^*}{\sigma_p^*} \right)} \quad (7b)$$

Herein,  $\varepsilon_y^*$  is the total strain at yield,  $\sigma_{UTS}^*$  is the engineering tensile strength and  $\varepsilon_{UTS}^*$  stands for uniform elongation. The graphs of the proposals of Ludwik, Hollomon and Swift show infinite gradients for  $\varepsilon \rightarrow 0$ . Contrarily, the Ramberg-Osgood representation features linear elastic behavior from the yield strength on down to the origin with the elastic modulus  $E$  as curve gradient. For large strains, all equations result in a small but finite curve gradient. That is to say, none of the approaches respects that at the ultimate point, which in the engineering stress-strain diagram corresponds to  $\sigma_{UTS}^*$ , both true and engineering stress are bounded and, hence, stress-strain curves must feature an extremum.

### Method of analysis

The underlying experimental stress-strain graphs were approximated exploiting Eqs. (4) – (7). A least square optimization was employed in order to fit the individual theoretical approaches to the test data. In the case of the Ludwik, Hollomon and Swift constitutive relation, stress-strain data was approximated for strains of 0.5% and greater. This was done in order to assure that no parent data is considered, which is either irrelevant or even detrimental for identification of plastic flow behavior and, hence, for strain hardening exponent assessment.

In this context it is important to notice that power-law approximations of Hollomon type always feature an infinite gradient in the origin and, thus, are inherently inaccurate in the range of small strains. This fact corroborates the procedure pursued.

### Pipe Material

Stress-strain data was analyzed for a total of six types of pipeline steel. The qualities of the material were ranging from API 5L grade X56 up to grade X100. The stress-strain behavior in longitudinal direction was analyzed on X80 and X100 line pipe steel.

**Transverse direction** Table 1 shows a list of pipe material taken in transverse direction along with corresponding mechanical parameters, notably those, which are important for assessing strain hardening behavior. The data goes back to an investigation carried out in 1995.

**Longitudinal direction** Table 2 summarizes pipe material taken in axial direction along with corresponding mechanical parameters. Per grade two different diameter-to-wall thickness ratios  $D/t$  were analyzed.

Table 1: Pipe material in virgin state (as formed): mechanical properties in transverse direction

N°	Grade	Y/T	$\varepsilon_{UTS}$ [ % ]
1	X56	0.70	15.8
2	X60	0.75	14.2
3	X65	0.80	13.0
4	X70	0.85	11.2
5	X100	0.94	5.3

Table 2: Pipe material in virgin state (as formed): mechanical properties in longitudinal direction

N°	Grade	Y/T	$\varepsilon_{UTS}$ [ % ]
1	X80	0.79	7.4
2	X80	0.81	7.5
3	X100	0.80	6.1
4	X100	0.80	5.6

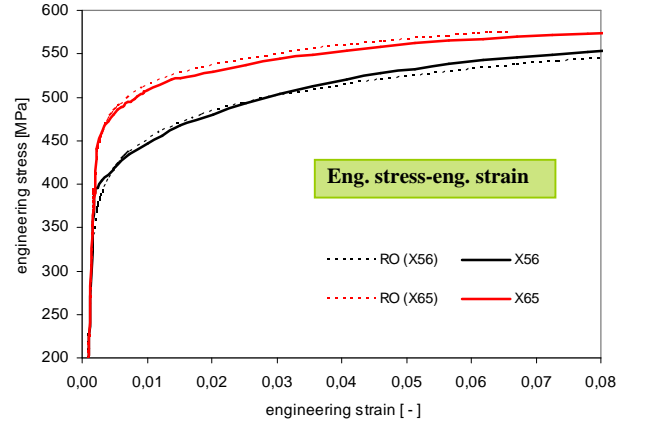


Fig. 3: Ramberg-Osgood representation of eng. stress-eng. strain behavior in transverse direction of X56 and X65 line pipe steel

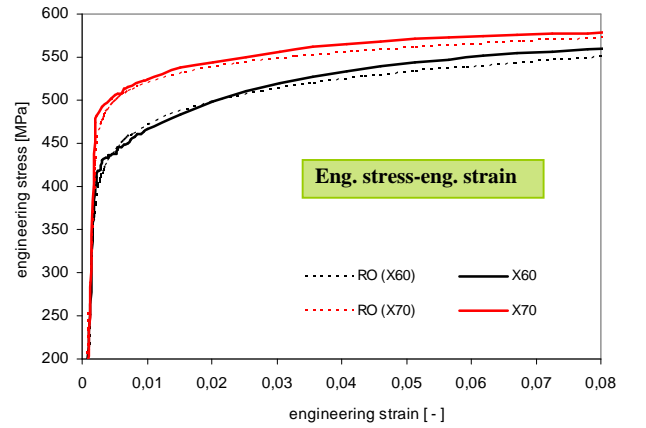


Fig. 4: Ramberg-Osgood representation of eng. stress-eng. strain behavior in transverse direction of X60 and X70 line pipe steel

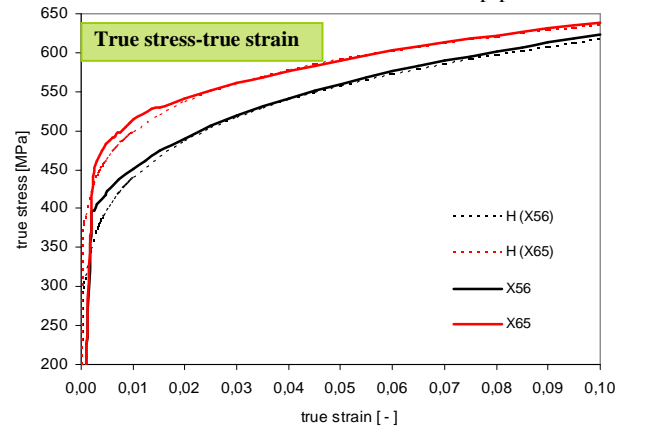


Fig. 5: Hollomon representation of true stress-true strain behavior in transverse direction of X56 and X65 line pipe steel

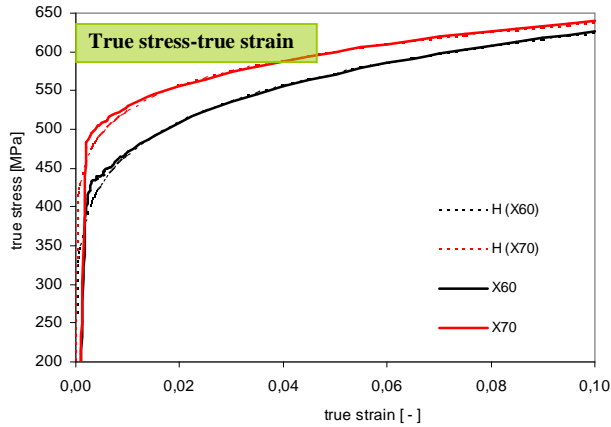


Fig. 6: Hollomon representation of true stress-true strain behavior in transverse direction of X60 and X70 line pipe steel

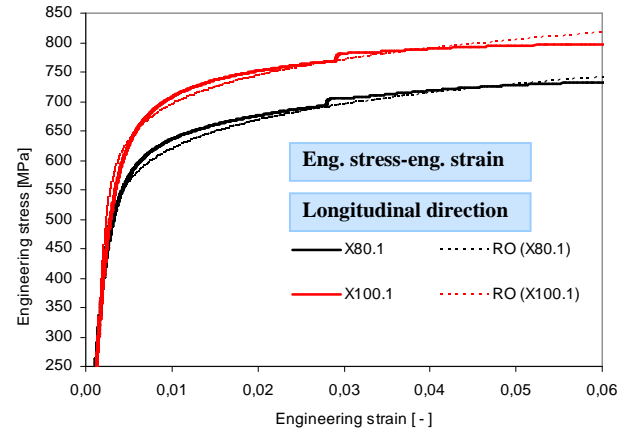


Fig. 7: Ramberg-Osgood representation of eng. stress-eng. strain behavior in longitudinal direction of X80 and X100 line pipe steel

### Graphical representation of results

Here, only a selection of stress-strain approximations is shown. Because of their particular significance for pipeline engineering practice, only stress-strain representations of Hollomon (“H”) and Ramberg-Osgood (“RO”) type are presented graphically.

Figs. 3-6 depict approximations of stress-strain behavior in transverse direction. For the sake of clarity, experimental stress-strain curves and their numerical representation of X56 and X65 pipeline steel were always combined in one diagram for each type of mathematical representation (Figs. 3 and 5). Likewise, steel types X60 and X70 were grouped in Figs. 4 and 6. In Table 3, strain hardening exponents are compiled for all constitutive equations presented above (Eqs. 4-7).

In Figs. 7 and 8 approximations of engineering stress-engineering strain behavior measured in longitudinal direction are displayed. Figs. 9 and 10 depict corresponding approximations of true stress-true strain behavior.

Table 3: Pipe material in virgin state (as fabricated): strain hardening exponents in transverse direction

Nº	Grade	Ludwik $n_L$	Hollomon $n_H$	Swift $n_S$	Ram.-Osg. $n_{RO}$
1	X56	0.1467	0.1467	0.1483	12.2
2	X60	0.1328	0.1259	0.1275	14.8
3	X65	0.1222	0.1054	0.1083	19.0
4	X70	0.1062	0.0846	0.0861	24.7
5	X100	0.0952	0.0554	0.0593	57.5

Table 4 summarizes work hardening exponents pertaining to pipe material listed in Table 2 and corresponding stress strain graphs shown in Figs. 7-10. Therein, only work hardening exponents of Ludwik, Hollomon and Ramberg-Osgood type are given.

Table 4. Pipe material in virgin state (as fabricated): strain hardening exponents in longitudinal direction

Nº	Grade	Ludwik $n_L$	Hollomon $n_H$	Ram.-Osg. $n_{RO}$
1	X80	0.1232	0.1020	11.5558
2	X80	0.1324	0.0850	13.8873
3	X100	0.1314	0.0910	13.1110
4	X100	0.1393	0.0964	12.2157

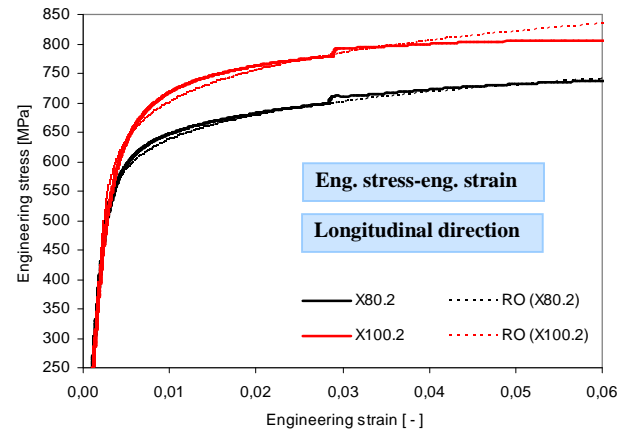


Fig. 8: Ramberg-Osgood representation of eng. stress-eng. strain behavior in longitudinal direction of X80 and X100 line pipe steel

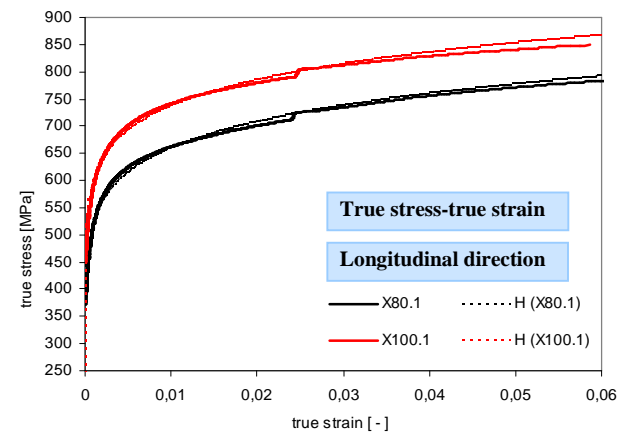


Fig. 9: Hollomon representation of true stress-true strain behavior in longitudinal direction of X80 and X100 line pipe steel

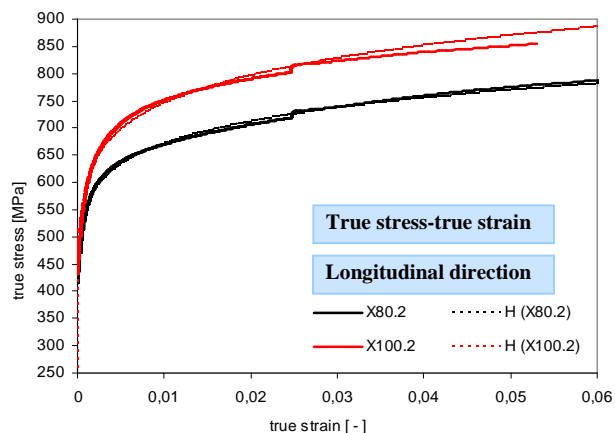


Fig. 10: Hollomon representation of true stress-true strain behavior in longitudinal direction of X80 and X100 line pipe steel

## Discussion

Based upon the results that were made throughout this research some general conclusions can be drawn. Comprehensive discussion of all constitutive equations towards representing stress-strain behavior and issues of refining modeling methodologies goes well beyond the scope of this paper. The findings can be summarized as follows:

- The Ludwik representation is prone to characterize well large plastic strains while still being sufficiently accurate in the vicinity of true yield strength. However, within our investigation, it did not add significantly to overall accuracy of the plastic flow curve representation
- Rather, the traces of Ludwik stress-strain approximations can be closely reproduced by the Hollomon approach for most line pipe steels.
- The Swift approach tends to represent high-strength line pipe steel best. Small discrepancies between experimental stress-strain curve and approximation are seen for strains smaller than 1%. However, these might be due to the necessity of estimating plastic pre-strains
- Ramberg-Osgood approximations supply appropriate descriptions of engineering stress-engineering strain data. With respect to the accuracy of representations there seems to be no particular difference between lower and higher strength material.
- Description by engineering stress-engineering strain curves by the Ramberg-Osgood constitutive equation leads to values of strain hardening exponent, which are conceptually different to those of true stress-true strain approaches. While strain hardening exponent of true-stress-true strain approaches is generally smaller than 0.5 strain hardening exponent of Ramberg-Osgood type models may go to infinity as underlying stress-strain information tends to trace perfectly elastic-perfectly plastic behavior

Comparing Tables 3 and 4 it becomes apparent that specimens machined in longitudinal direction feature stress-strain behavior, which is convenient for strain based design. Yield-to-tensile ratio  $Y/T$  and Ramberg-Osgood work hardening exponent  $n_{RO}$  are even lower than those upraised in transverse direction.

## SIMPLIFIED METHOD FOR COMPUTING STRAIN HARDENING EXPONENTS

### General

In addition to providing information on stress and strain, pipe manufacturers can actively support the design process by supplying strain hardening exponents. This section lays out a method for estimating strain hardening exponents of Hollomon type for transverse

direction. Historically, a low yield-to-tensile ratio was considered to provide sufficient ability for plastic deformation and hence a necessary margin of safety against ultimate failure. In reality however, the effect of yield-to-tensile ratio on overall mechanical material and structural behavior is very complex to assess. This is because there seem to be many implications with other material characteristics such as the presence of a Lüders plateau, fracture toughness and the physical nature of strain hardening. Besides,  $Y/T$  merely addresses singular points of individual stress-strain behavior, namely the onset of yielding and material tensile strength. For some mechanical analyses this might be insufficient.

Despite all implications with other material characteristics, experimental evidence has shown that both yield and tensile strength of a material have significant effect on impending failure of pipelines. It is anticipated that, inherently, the yield-to-tensile ratio is closely related to strain hardening of pipeline material. Taking this as a natural starting point, the next section theoretically explores the possibilities of correlating strain hardening exponents and  $Y/T$  based on a proposal of Zhu and Leis (2004). As will be seen at a later juncture, the Hollomon approach will emerge as a successful, yet simple, approach for achieving this goal under the sole condition that the material obeys power-law plasticity.

### Strain hardening exponent as a function of $Y/T$

Due to the presence of cold forming within the UOE production route the stress-strain diagram of current Europipe material features a smooth trace in transverse direction. This fact permits true stress-true strain curves be reproduced by power-law approximations without loss of crucial constitutive information. The simplest form of a power law curve is the one of Hollomon, which proved to be an excellent representation of experimental true stress-true strain curves in the regime of uniform plastic deformation. Moreover, it is well-suited for plastic collapse analysis of pipelines.

Until the maximum load is attained plastic flow develops uniformly. In this regime of large uniform deformation, true stress  $\sigma$  and true strain  $\varepsilon$  can be expressed using engineering stress  $\sigma^*$  and strain  $\varepsilon^*$ :

$$\sigma = \sigma^* (1 + \varepsilon^*), \quad \varepsilon = \ln(1 + \varepsilon^*) \quad (8)$$

Substitution of Eqs. (8) in to the Hollomon power law (5) and solving for the true stress gives:

$$\sigma = C_H \frac{[\ln(1 + \varepsilon^*)]^{n_H}}{1 + \varepsilon^*} \quad (9)$$

Generally, localization of deformation, that is to say necking, begins when the maximum force is attained during tensile testing of a ductile material. At this point, engineering stress and engineering strain take their ultimate values  $\sigma_{UTS}^*$  and  $\varepsilon_{UTS}^*$ . After the point of necking initiation, the engineering stress decreases as the engineering strain increases. Thus, the instability condition is defined by (Zhu and Leis, 2004a, b, Law et al., 2004):

$$\frac{d\sigma^*}{d\varepsilon^*} = 0 \quad (10)$$

Substitution of Eq. (9) into Eq. (10) and assessing proves that the Hollomon strain hardening exponents equals:

$$n_H = \ln(1 + \varepsilon_{UTS}^*) = \varepsilon_{UTS}^* \quad (11)$$

where  $\varepsilon_{UTS}$  is the true ultimate strain at necking initiation. If the corresponding true ultimate stress is denoted by  $\sigma_{UTS}$ , from Eqs. (5a) and (11) one obtains:

$$\sigma_{UTS} = C_H (\varepsilon_{UTS})^{n_H} = C_H n_H^{n_H}. \quad (12)$$

In the following the subscript “H” is omitted for simplicity. Solving this for the strength coefficient yields:

$$C = \frac{\sigma_{UTS}}{n^n} = \frac{\sigma_{UTS}^* (1 + \varepsilon_{UTS}^*)}{n^n}. \quad (13)$$

Because  $\ln(1 + \varepsilon_{UTS}^*) = n$  there is  $(1 + \varepsilon_{UTS}^*) = e^n$ . Using this intermediary result, Eq. (13) takes the form of Eq. (5b):

$$C = \left(\frac{e}{n}\right)^n \sigma_{UTS}^*.$$

If the “yield point” ( $\varepsilon_y | \sigma_y$ ) of the true stress-true strain relation, where  $\varepsilon_y = \ln(1 + \varepsilon_y^*)$  and  $\sigma_y = \sigma_y^* (1 + \varepsilon_y^*)$ , is on the power law curve as given by Eq. (5a), one may write:

$$\sigma_y^* (1 + \varepsilon_y^*) = C [\ln(1 + \varepsilon_y^*)]^n, \quad (14)$$

and further, employing relation (5b):

$$\sigma_y^* (1 + \varepsilon_y^*) = \left(\frac{e}{n}\right)^n \sigma_{UTS}^* [\ln(1 + \varepsilon_y^*)]^n. \quad (15)$$

From Eq. (15) one may extract:

$$\frac{\sigma_{UTS}^*}{\sigma_y^*} = (1 + \varepsilon_y^*) \left[ \frac{n}{e \ln(1 + \varepsilon_y^*)} \right]^n, \quad (16)$$

In fact, Eq. (16) establishes a functional relationship between the strain hardening exponent and the yield-to-tensile ratio. Denoting, as usual,  $\sigma_{UTS}^*$  by  $T$  and  $\sigma_y^*$  by  $Y$  and respecting  $\varepsilon_y^* \ll 1$ , one may simplify as follows:

$$\frac{1}{\left(\frac{Y}{T}\right)} = (1 + \varepsilon_y^*) \left[ \frac{n}{e \varepsilon_y^*} \right]^n \quad (17)$$

According to German standards, the yield strength ( $R_{p0,2}$ ) is commonly defined at the 0,2% plastic offset strain. Hence, the total strain at yield is then:

$$\varepsilon_y^* = 0,002^* + \frac{R_{p0,2}}{E} \quad (18)$$

It is clear from Eq. (15) that  $\varepsilon_y^*$  must depend upon the stress-strain characteristic of the material under investigation. There is no unique solution covering all possible combinations of yield-to-tensile ratio and yield strength. A practical solution of removing this dependence consists

in deriving an average absolute value  $R_{p0,2}/E$  from the lower and upper limit case of yield strength  $R_{p0,2}$ , applying to UOE pipe production, and substituting it into Eq. (14). This certainly is an approximation, but as will be shown later on, it provides sufficiently accurate estimates of strain hardening exponent.

Within the scope of this investigation, steel has been considered ranging from grade X56 up to grade X100. The yield strengths were 395 MPa and 786 MPa for steel grade X56 and X100 respectively. Correspondingly, one derives strains at yield of  $\varepsilon_y^* = 0,0039$  and  $\varepsilon_y^* = 0,00576$  respectively. The average of total strain at yield for grade X56 and X100 then amounts to  $\varepsilon_y^* = 0,00483$ . Substituting this into Eq. (14) and assessing gives:

$$\frac{Y}{T} \approx 0,995 \left( \frac{0,01313}{n} \right)^n \quad (19)$$

When plotting the relationship  $Y/T$  vs.  $n$  (17) for  $\varepsilon_y^* = 0,0039$ ,  $\varepsilon_y^* = 0,00576$  and the mean value  $\varepsilon_y^*,_{mean} = 0,00483$ , then it is seen that the latter one firmly interpolates between the boundaries correlating with moderate and extreme values of yield strength, see Fig. 11. Likewise, the graphs in Fig. 11 give indication that, intrinsically, the strain hardening exponent may not just be a function of  $Y/T$  alone but of the yield stress  $Y$  as well. Furthermore, close inspection of the graphs reveals that the curves do not reach down to  $n = 0$  for  $Y/T \rightarrow 1$ . This, at first sight, surprising phenomenon is to be attributed to the fact that even for a perfectly elastic-plastic engineering stress-engineering strain diagram the associated true stress-true strain diagram has a finite slope not equal to zero. The horizontal grey line in Fig. 12 highlights this phenomenon.

Since Eqs. (17) and (19) are implicit in nature, these cannot be solved for the strain hardening exponent  $n$  directly. In order to generate an explicit expression for the strain hardening exponent, it is attempted to represent Eq. (19) by a polynomial of order two. It was found that

$$14,369 n^2 + 0,842 n + 0,995 = \frac{1}{Y/T} \quad (20)$$

adequately approximates Eq. (19). Eq. (20) can be easily solved for the strain hardening exponent, to give:

$$n = -0,0293 + \sqrt{\frac{0,0696}{Y/T} - 0,0683}. \quad (21)$$

Relationship (21) has been evaluated and the corresponding graph depicted in Fig. 12, along with the plot according to Eq. (19) and the data of Hollomon strain hardening exponent  $n_H$ , taken from Table 3. It is to be noted that each data point of Hollomon strain hardening exponent – represented as circular point in Fig. 12 – was determined based on the best individual fit to the underlying true stress-strain curve received from transverse tensile testing on round bar specimens. Thus, these did not originate from bare theoretical consideration. Comparing the final theoretical approximation (21) and the results from curve fitting reveals potential and efficacy of this approach. Nonetheless, there is still some inaccuracy for  $Y/T \geq 0,93$  where the results obtained from best fit analysis switch their locus from underneath to above the theoretical curve. This might be due to specific architecture and composition of material microstructures (uncommon alloying elements, etc.) associated with such elevated yield-to-tensile ratios. From the fact that for yield-to-tensile ratios  $Y/T \geq 0,93$  actual values of strain hardening exponent have their locus clearly above the theoretical curve, it is inferred that there is still dormant potential for improvement of circumferential elongation of high-strength line pipe.

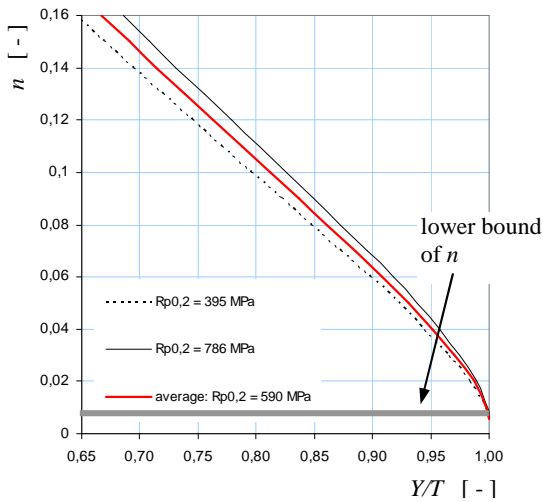


Fig. 11: Strain hardening exponent  $n$  vs. yield-to-tensile ratio  $Y/T$ , Eq. (19)

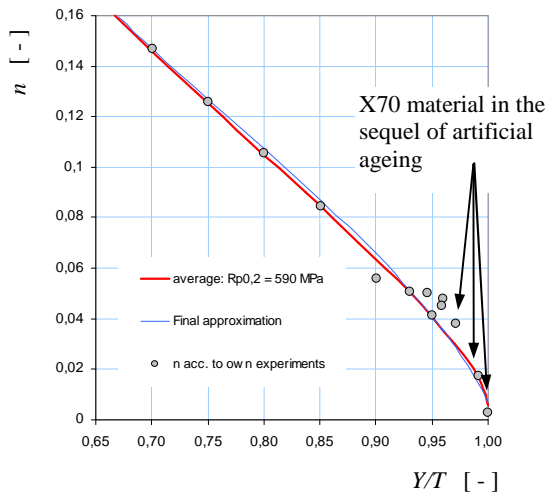


Fig. 12: Strain hardening exponent  $n$  vs. yield-to-tensile ratio  $Y/T$ , Eq. (21)

## CONCLUSIONS

Limit State Design calls for application of advanced methods of analyses, including advanced material solutions. This requires exact representations of constitutive behavior of line pipe steel and structural pipe behavior also beyond the onset of yielding, until the ultimate limit state marked by bursting. The load bearing capacity, once yielding has started, is strain based. One essential component of Strain Based Design is the material's strain hardening behavior, which may be limited for line pipe steels of higher grades. Here the possible contribution of manufacturer comes into play: Next to basic parameters of the stress-strain-behavior like uniform elongation, yield strength, tensile strength and yield-to-tensile ratio knowledge of strain hardening exponent is useful for any strain based assessment of safety. Strain capacity and, thus, strain hardening exponent can be relevant in axial as well as in circumferential direction, depending on the type of loading (pressure containment only or additional presence of external loads). In this context, representative graphs of uni-axial stress-strain behavior

were shown for both circumferential and longitudinal direction for a wide range of steel grades. Furthermore, experimental stress strain information was approximated using well-accepted constitutive approaches and corresponding work hardening parameters compiled.

A procedure for strain hardening exponent estimation was developed for stress-strain behavior in transverse direction of UOE line pipe. The mathematical approach supposes validity of the Hollomon power law approximation and declares yield-to-tensile  $Y/T$  ratio as the leading parameter. The correlation was evaluated exactly for two sorts of steel (X56 and X100) featuring about the limit levels (lower and upper bound) of yield strength of today's UOE pipe production. In so doing, it became apparent that, indeed yield-to-tensile ratio is prevailing, but not the only parameter controlling strain hardening exponent. Specifically, yield strength might exert some additional effect. Defining an average value for the complete range of yield strength of current Europe pipe production conveniently decouples strain hardening exponent from yield strength.

Comparing with results from best fit analysis showed that the final approximate expression is simple to operate and efficient for a wide range of pipeline steel material.

## REFERENCES

- Bowker, J.T., Gianetto, J.A., Shen, G., Tyson W. and Horsley, D. (2006). "Cross-Weld Tensile Properties of Girth Welds for Strain Based Designed Pipeline" Int Pipeline Conf, Calgary, Canada, IPC, Paper 10400.
- CSZ Z662-03. Canadian Standards Association (2003). "Oil and Gas Pipeline Systems".
- Hollomon, J.H. (1949). "Tensile Deformation". *Transactions of the American Institute of Mining, Metallurgical and Petroleum Engineers*, Vol 16, pp 268–290.
- Martin, R. (2006). "Investment in Oil and Gas Filed Materials Technology - The Key to a Secure Energy Supply". *Energy Materials*, Vol 1, pp 11-13.
- Mohr, W. (2006). "Strain Based Design for Materials with HAZ Softening" Int Pipeline Conf, Calgary, Canada, IPC, Paper 10424.
- Law, M., Bowie, G., Fletcher, L. (2004): Burst Pressure and Failure Strain in Line Pipe, Part 3, Failure Pressure Calculated by the Method of Plastic Instability. *The Journal of Pipeline Integrity*, Vol. 3, pp 107-111
- Ludwik, P. (1909). *Elemente der Technologischen Mechanik*, 1<sup>st</sup> edition, Springer.
- Ramberg, W., Osgood, W.R. (1943). "Description of Stress-Strain Curves by Three Parameters". *National Advisory Committee for Aeronautics (NACA), Technical Note N° 902*.
- Thomas, S. (2001): *Konstitutive Gleichungen und Numerische Verfahren zur Beschreibung von Verformung und Schädigung*. Dissertation, Technische Universität Darmstadt, Darmstadt
- Zhou, J., Horsley, D. and Rothwell B. (2006). "Application of Strain-Based Design for Pipelines in Permafrost Areas". Int Pipeline Conf, Calgary, Canada, IPC, Paper 10054.
- Zhu, X.K., Leis, B.N. (2004a): Strength Criteria and Analytical Predictions of Failure Pressure in Corroded Line Pipes. *International Journal Offshore and Polar Engineering*, Vol. 14, pp 125-131.
- Zhu, X.K., Leis, B.N. (2004b): Accurate Prediction of Burst Pressure for Linepipes. *The Journal of Pipeline Integrity*, Vol. 3, pp 195-206